Experimental validation of an isolated resonant converter for auxiliary systems in a train

J. Giles[1], A. Rodríguez[1], M. M. Hernando[1], J. Sebastián[1], B. Zelaa[2], J. Aguirre[2], A. Castro[2], J. M. Bermejo[2] and D. Ortega[2]
[1]University of Oviedo. Power Supply Systems Group
Campus de Viesques s/n, 33204 Gijón. Spain
[2]Ingeteam Power Technology S.A
48170 Zamudio. Vizcaya. Spain
Tel.: +34 – 985 18 25 78
E-Mail: gilesjoan@uniovi.es
URL: www.uniovi.es[1] www.ingeteam.com[2]

Acknowledgments

This work has been funded by the "Fundación para la Investigación Científica y Técnica" (FICYT) through project SV-PA-21-AYUD/2021/51931, by the European Commission HORIZON and KDTJU under the project POWERIZED GA No 101096387 and by the Spanish Ministry of Science and Innovation under grant MCINN-23-PCI2022-135021-2.

Keywords

«Railway auxiliary systems», «Resonant converter SRC», «High power prototype».

Abstract

This paper presents preliminary experimental results of a high-power resonant converter as a part of the auxiliary systems of a train. A series resonant converter is used developed and tested, since it has interesting characteristics for this type of applications, such as galvanic isolation, good power density and high efficiencies.

Introduction

In recent years, the electrification of mobility has grown rapidly, including railway systems, which are optimizing their electrical systems, seeking to have smaller, lighter and more efficient systems.

Nowadays, in railway systems, the electrical power is transferred to the train through a catenary placed on top of the train. The catenary can be either dc or ac, and can have different voltages. The train has the necessary power electronics to supply its two main systems: the traction system and the auxiliary system. Depending on whether the train has an independent or integrated topology, the traction system and the auxiliary system may share the same dc bus.

However, in accordance with the UNE EN 50163 standard the voltage of the catenary may change widely generating variations in the high-power dc bus voltage which affects the power electronics of the auxiliary systems [1]. The auxiliary systems must supply electrical power to the electrical and electronic equipment on the train, such as lighting systems, compressors, heaters, fans, pumps, air

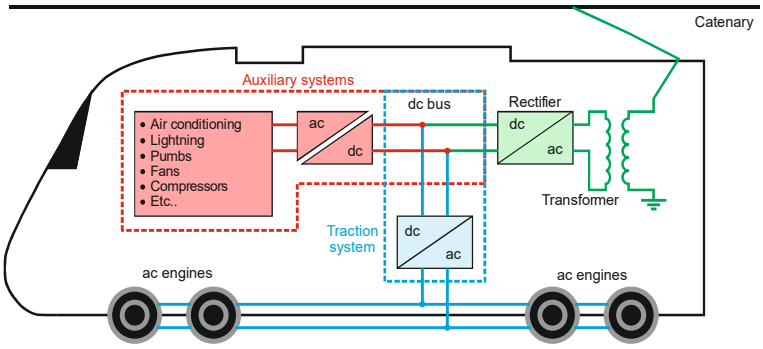

Fig. 1: Example of the electrical system of a train with an ac catenary and with an integrated topology for its traction and auxiliary systems.

conditioners, etc. In general, auxiliary systems demand an electrical power in the range of 20 kW to 200 kW, depending on the type of train and the loads installed on it.

An auxiliary system consists of a dc-ac power converter, which for safety reasons must have galvanic isolation in some of its stages [2]. Likewise, the converter must take into account the variations in the input dc bus voltage, as well as, at the output it must provide a three-phase ac voltage.

An example of an electrical system of the train with an integrated topology is shown in Fig. 1. At the top is an ac catenary, then a transformer adapts the voltage so that a rectifier can convert the ac voltage to a dc voltage, thus generating the high-power dc bus. Then, the high-power dc bus is connected to the traction system, which energizes the traction motors, and the auxiliary system that feeds all the auxiliary loads.

In recent years, different converter topologies have been studied for the auxiliary systems. In general, the system is divided into two converters to try to increase its power density. A first dc-dc converter, in which galvanic isolation is provided, followed by a dc-ac converter (inverter). The inverter is not analyzed in this paper. The design of the dc-dc converter implies a thorough study due to the different needs of the system, such as galvanic isolation, good power density, good heat dissipation and relatively good efficiencies.

In this paper, a qualitative comparison of different isolated converter topologies, some with pre-regulator converters and others with Silicon Carbide (SiC) semiconductors, is performed. Moreover, an experimental setup is proposed to test a high-power resonant converter prototype. The developed converter is tested in the proposed setup in simulation and experimentally in order to compare the results and validate the expected performance.

Qualitative comparison of topologies for the dc-dc stage of the auxiliary converter

In recent years, different topologies for dc-dc converters in railway auxiliary systems have been analyzed. The full-bridge (FB) converter is one of the preferred topologies for medium and high-power converters [3]. However, this converter has hard switching, which results in system losses and reduced maximum switching frequency. Also, several solutions based on auxiliary circuits or switching techniques have been proposed for this converter [4]. However, installing more components decreases the power density and increases the complexity of the converter, and often such solutions do not justify the use of the converter for this type of applications [5].

The Single Active Bridge (SAB) and Dual Active Bridge (DAB) converters are well known converters in this type of applications. The SAB is used in applications where the power flow is unidirectional and the DAB mainly in applications with bidirectional power flow. Both converters feature galvanic isolation and high-power density [6], thanks in part to their soft switching. However, under certain load conditions the soft switching can be lost. In addition, voltage variations cause the transformer rms current to increase dramatically [7]. The aforementioned affects the performance of such converters, thus limiting their use in this type of applications.

Different topologies of resonant converters have been proposed for the use of auxiliary converters in trains, such as series, parallel and parallel series, LLC and LCC topologies [8], [9]. Resonant converters have interesting features for this type of systems, such as galvanic isolation, high efficiency and good power density [2]. Resonant converters have the best efficiency when the resonant frequency is equal to the switching frequency [8]. However, if the switching frequency is changed, the performance of the resonant converter is reduced. Therefore, depending on the input voltage variations the switching frequency of the converter can vary drastically, decreasing its performance.
Furthermore, different topologies of isolated converters, isolated converters in combination with pre-regulators, as well as the use of silicon carbide (SiC) semiconductors have been proposed [1], [6], [10], [11]. Using converters as pre-regulators allows improving the performance of the converter with isolation, however, the number of components is increased. Likewise, using SiC semiconductors allows to increase the switching frequencies, but the topology cost increases considerably.
Therefore, in order to have a better comparison of the different topologies, a study was carried out

Table I: Qualitative comparison of different topologies for isolated dc-dc converters in auxiliary converters.

Topology	Maximum switching frequency [kHz]	Added inductors	Cost	Transformer complexity	Control complexity
SAB					
SAB	1	1			
SiC+SAB	7	0			
Boost+SAB	1 (Boost) + 2.5 (SAB)	1			
Buck+SAB	1 (Buck) + 4 (SAB)	1			
FB					
FB	2.5	1			
SiC+FB	10	1			
Boost+FB	1 (Boost) + 4 (FB)	1			
Buck+FB	1 (Buck) + 8 (FB)	1			
Resonant					
Series Resonant	0.5	1			
Buck+Series Resonant	1 (Buck) + 10 (Resonant)	0			
Boost+ Series Resonant	1 (Boost) + 7 (Resonant)	0			

with specific system parameters. A nominal input voltage on the dc bus of 3000 V, an output voltage of 800 V and a maximum power of 200 kW were established. Table I shows the most relevant comparative results. SAB, FB and series resonant topologies were compared, some of them with pre-regulator converters connected between the catenary and the isolated converter. Furthermore, in order to increase the switching frequency, the use of SiC semiconductor devices is evaluated.

Table I consists of six columns, which describe the most relevant results of the comparison of the mentioned topologies. In the table, the green cells represent a benefit, the yellow cells an intermediate benefit and the red cells a deficit of the topology. The first column describes the topology evaluated, whether it has a pre-regulator or not, or whether it uses SiC semiconductors. The switching frequency is key to topology selection, as it determines the size of the reactive components. Therefore, the second column shows the maximum frequency at which the isolated converter could be operated, as well as the frequency of the pre-regulator. It is important to mention that all the evaluated converters have an inductor in their topology. Depending on the switching frequency, this inductor can be of such a relatively small value that it can be integrated in the converter transformer. Therefore, the third column shows whether the converter inductor can be the transformer leakage inductance or whether it is necessary to add one. The fourth column shows the average cost of the converter, which takes into account the increased cost due to the use of a pre-regulator and SiC devices. Some topologies involve considering a larger number of parameters when designing the transformer, which makes the design more difficult. Finally, some converters imply a higher complexity in their control when implemented, which is considered in the sixth column.

According to Table I, topologies with SiC devices achieve good switching frequencies, however, they imply relatively high costs, so they are not a viable option. On the other hand, FB + pre-regulator topologies have relatively good switching frequencies, however, they need an additional inductor in their output, in addition, the design of its transformer implies a certain difficulty. Finally, the series resonant topologies + pre-regulator have relatively high switching frequencies, so it is the case that its inductor can be easily included in the transformer, in addition, they involve low costs, its transformer is relatively simple to design (the resonant frequency can be adjusted with the resonant capacitor) and in general it is easy to implement its control.

Experimental setup to test the resonant converter prototype

According to previous section, a series resonant converter with pre-regulator is considered the best option. The pre-regulator converter has the function of regulating the voltage at the input of the resonant converter, which allows the resonant converter to work close to at the resonant

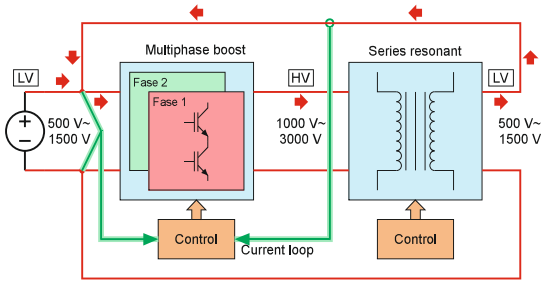

Fig. 2: Block diagram of the proposed solution.

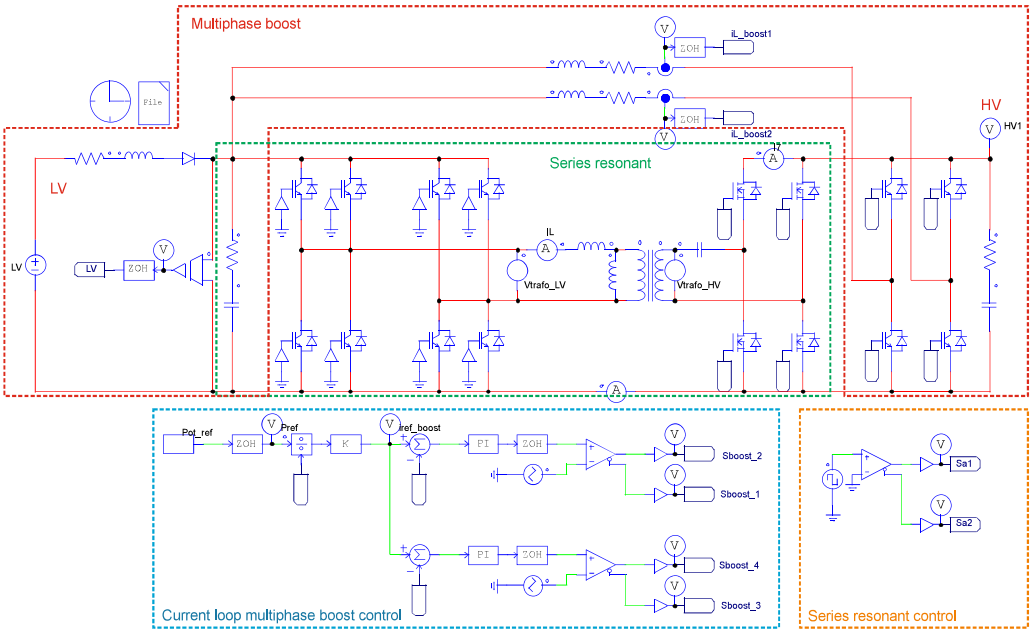

Fig. 3: Schematic diagram of the proposed solution.

frequency with a very good performance, even at medium frequency. Therefore, a closed-loop pre-regulator converter is connected to an open-loop series resonant converter.

In this paper, the simulation and experimental validation of a high-power series resonant converter prototype is performed. As a high voltage source is not available in the laboratory, it is necessary to boost the voltage of a low voltage laboratory source by means of a pre-regulator to experimentally test the resonant converter close to its nominal voltage condition. Fig. 2 shows the block diagram of the proposed solution for experimental validation. Fig. 2 shows the laboratory source of relatively low voltage (LV) connected to a multiphase boost converter of two interleaved phases, this converter raises the LV to a high voltage (HV), which supply the resonant converter. Then, the output of the resonant converter is connected to the LV bus, this is done to recirculate the energy and not to waste electrical power in the tests.

The multiphase boost converter regulates the output current of the resonant converter, while the resonant converter is in open loop. The values of voltage, power and switching frequencies of the system are:

- LV source voltage of 1000 V, with minimum voltages of 500 V and maximum voltages of 1500 V.
- Switching frequency of 800 Hz for the two-phase interleaved boost converter (each phase is phase-shifted 180°).
- Nominal input voltage of the resonant converter of 2000 V, with minimum voltages of 1000 V and maximum voltage of 3000 V, at a switching frequency of 7 kHz.

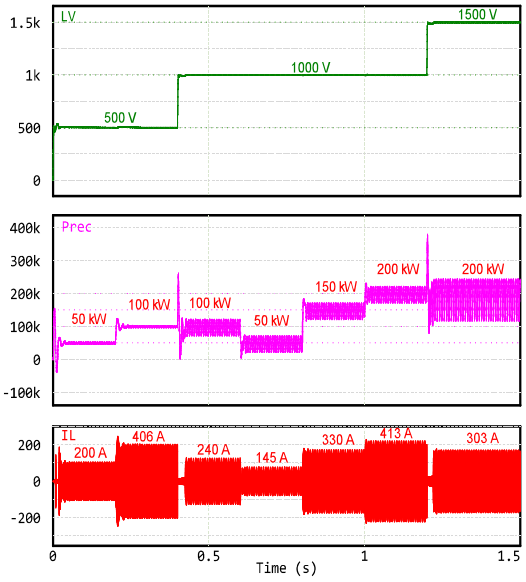

Fig. 4: Simulation dynamic response of the proposed system for voltage and load changes. The input voltage is represented by the green waveform, the recirculation power by the purple waveform and the resonant current of the resonant converter by the red waveform.

- A maximum continuous power of 200 kW, with a maximum peak power of 240 kW.

Simulation results

Simulations were carried out with PSim software, taking into consideration most of the characteristics of the semiconductors and magnetics to achieve simulations as close to the implementation as possible.
Fig. 3 shows the schematic diagram of the simulation, as well as a division into colored blocks of the stages of the proposed solution. The red block corresponds to the multiphase boost converter. The LV corresponds to the input voltage of the laboratory source and HV to the input voltage of the resonant converter. The green block corresponds to the resonant converter, where its output is connected to LV to recirculate the energy. Finally, the blue block corresponds to the control loop of the multiphase converter and the orange block to the control of the resonant converter.

In order to validate the dynamics of the proposed solution, a simulation of the complete system was carried out. Changes in the value of LV and in the recirculation power (load changes) were applied. Fig. 4 shows the variations of HV, recirculation power (Prec) and resonance current (IL). The figure shows that regardless of the voltage variations, the system properly regulates the demanded power.

Fig. 5, Fig. 6 and Fig. 7 show the waveforms of the resonant current (IL), the conduction current (Ia1) and the collector-emitter voltage of an IGBT (VCE) of the resonant converter, at different operating conditions. Fig. 5 corresponds to a test at 50kW, Fig. 6 at 200 kW and Fig. 7 at 240 kW. All simulations are performed with a LV of 1000 V and a HV of 2000 V.

The IL current waveforms of all tests are relatively similar in shape (because the resonant converter is working in open loop close to the resonant frequency), although not in magnitude.

An interesting difference in Ia1 waveforms is observed. In the 50 kW test, the required current to obtain soft switching is noticeable at IGBT turn-on. However, this current peak, although present, is not very noticeable in higher power tests.

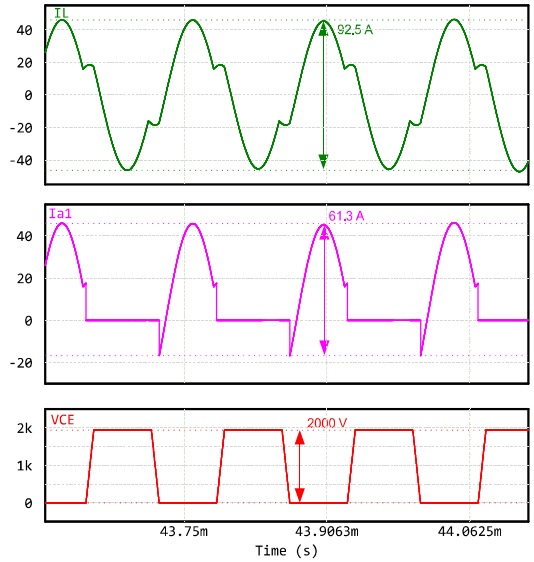

Fig. 5: Simulation with a voltage in LV of 1000 V at a power of 50 kW in the resonant converter. The resonant current (IL) is represented in green, the IGBT conduction current (Ia1) in purple and the collector-emitter voltage of an IGBT (VCE) in red.

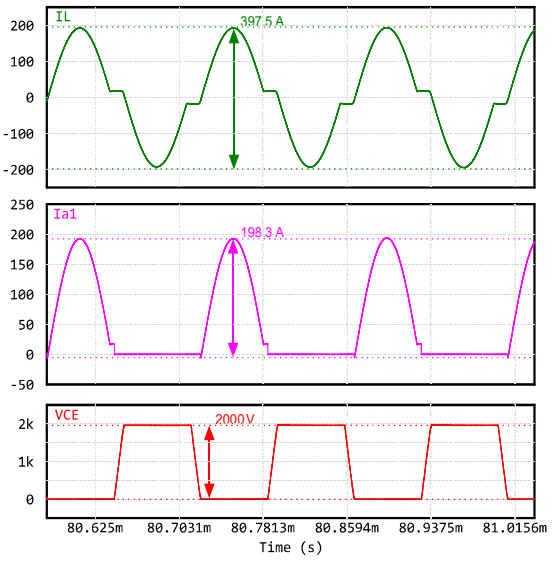

Fig. 6: Simulation with a voltage in HV of 1000 V at a power of 200 kW in the resonant converter. The resonant current (IL) is represented in green, the IGBT conduction current (Ia1) in purple and the collector-emitter voltage of an IGBT (VCE) in red.

In addition, Fig. 8. shows the waveforms of the phase currents (iL_boost1 and iL_boost2) of the two-phase boost converter. The test corresponds to a voltage of 500 V at LV and a power of

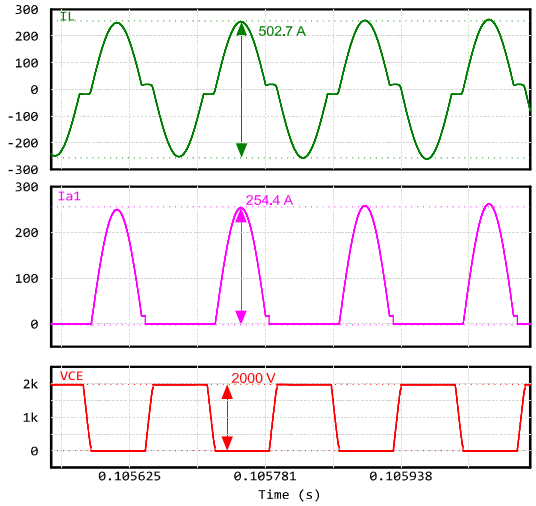

Fig. 7: Simulation with a voltage in HV of 1000 V at a power of 240 kW in the resonant converter. The resonant current (IL) is represented in green, the IGBT conduction current (Ia1) in purple and the collector-emitter voltage of an IGBT (VCE) in red.

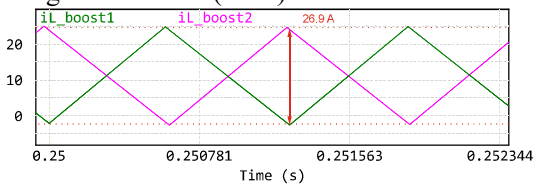

Fig. 8: Waveforms of the currents per phase (iL_boost1 and iL_boost2).

10 kW. The figure shows that the currents iL_boost1 and iL_boost2 are phase-shifted 180°.

Experimental results

The resonant converter prototype and the experimental tests were carried out at the company Ingeteam in Zamudio, Spain, since it has the necessary capacity to supply the electrical power to the prototype. Fig. 9 shows a picture of the implemented prototype. The figure shows the transformer of the resonant converter and the inductors of the multiphase boost converter, in addition, the location of the HV and LV buses is indicated. In the following sections, the experimental results are shown and compared with the simulation results.

In Fig. 10, Fig. 11, and Fig. 12 the waveforms of the resonant current, collector-emitter voltage and conduction current of an IGBT of the resonant converter are shown. The results in these figures are comparable with the simulation results in Fig.

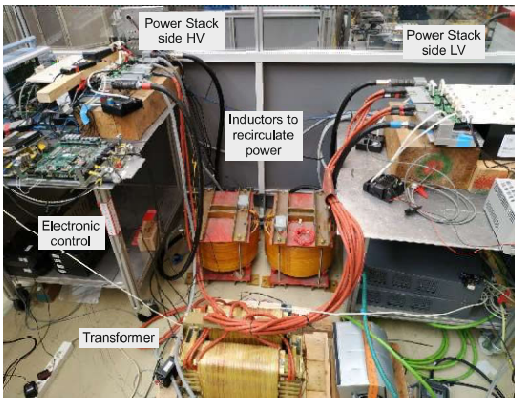

Fig. 9. Picture of the experimental prototype.

5, Fig. 6, and Fig. 7, respectively, since they have the same simulation and implementation parameters. Similarly, the soft switching of the resonant converter can be observed in all three tests. Likewise, all tests have similar waveforms in simulation and implementation. And although there are differences in the magnitudes, the differences are minimal with respect to the system power. In the tests, 85 mJ of turn-off energy has been measured, which at 7 kHz are almost 600 W of switching losses.

In addition, Fig. 13 shows the waveforms of the currents of each phase of the boost converter. The test is comparable with the simulation in Fig. 8.

Conclusions

In this paper, a solution for the isolated dc-dc converter responsible for supplying electrical power to the auxiliary systems of a train is proposed. The proposed solution was an open-loop series resonant converter in cascade with a closed-loop pre-regulator converter.

The series resonant converter shows relatively good performance at various operating points, especially when its switching frequency works close to the resonance frequency. This operation has been validated thanks to the development of a high-power prototype of the resonant converter and an experimental setup. Moreover, simulation and experimental results are very similar in shape and magnitude.

After the preliminary experimental tests presented in this paper, the analysis of the operation of the resonant converter is being performed at different operating points, such as with different values of dead time, operation at start-up, with power peaks, etc.

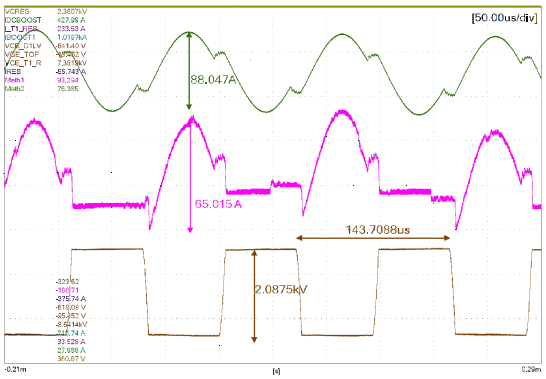

Fig. 10: Experimental results with a voltage in LV of 1000 V and a power of 50 kW. The resonant current is represented in green, the IGBT conduction current in purple and the IGBT collector-emitter voltage in brown.

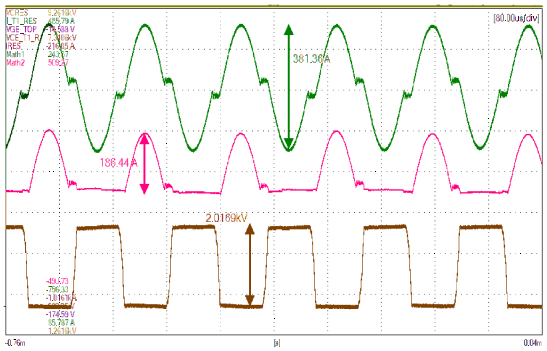

Fig. 11: Experimental results with a voltage in LV of 1000 V and a power of 200 kW. The resonant current is represented in green, the IGBT conduction current in purple, and the IGBT collector-emitter voltage in brown.

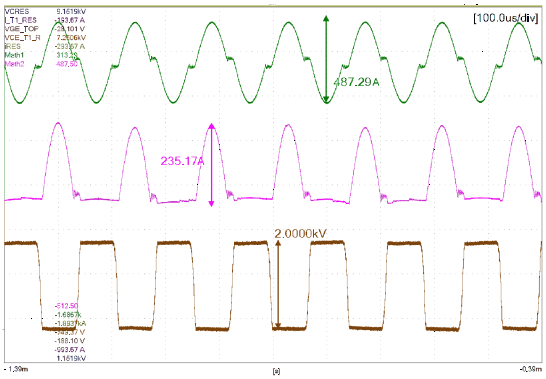

Fig. 12: Experimental test with a voltage in LV of 1000 V and a power of 240 kW. The resonant current is represented in green, the IGBT conduction current in purple, and the IGBT collector-emitter voltage in brown.

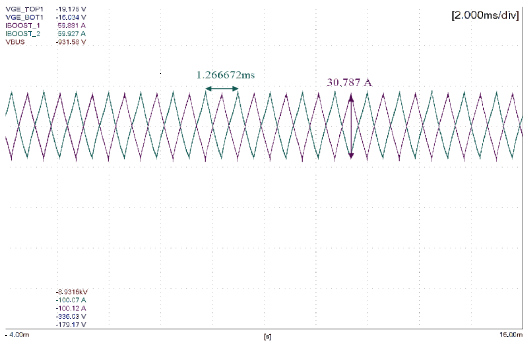

Fig. 13: Experimental waveforms of the inductor currents per phase of the two-phase multiphase converter.

References

[1] M.-A. Ocklenburg, M. Döhmen, X.-Q. Wu, M. Helsper, «Next generation DC-DC converters for Auxiliary Power Supplies with SiC MOSFETs», 2018 IEEE International Conference on Electrical Systems for Aircraft, Railway, Ship Propulsion and Road Vehicles & International Transportation Electrification Conference (ESARS-ITEC), 2018, pp. 1-6. doi: 10.1109/ESARS-ITEC.2018.8607463.

[2] A. Maerz M.-M. Bakran, «Designing a low weight low loss auxiliary converter for railway application», PCIM Europe 2014; International Exhibition and Conference for Power Electronics, Intelligent Motion, Renewable Energy and Energy Management, 2014, pp. 1-8.

[3] R. W. A. A. De Doncker, D. M. Divan, M. H. Kheraluwala, «A three-phase soft-switched high-power-density DC/DC converter for high-power applications», IEEE Trans Ind Appl, vol. 27, n. 1, pp. 63-73, 1991, doi: 10.1109/28.67533.

[4] V. R. K. Kanamarlapudi, B. Wang, N. K. Kandasamy, P. L. So, «A New ZVS Full-Bridge DC–DC Converter for Battery Charging With Reduced Losses Over Full-Load Range», IEEE Trans Ind Appl, vol. 54, n. 1, pp. 571-579, 2018, doi: 10.1109/TIA.2017.2756031.

[5] N. H. Baars, H. Huisman, J. L. Duarte, J. Verschoor, «A 80 kW isolated DC-DC converter for railway applications», 2014 16th European Conference on Power Electronics and Applications, 2014, pp. 1-10. doi: 10.1109/EPE.2014.6910741.

[6] Y. Li, A. Junyent-Ferré, P. D. Judge, «A Boost-Full-Bridge-Type Single-Active-Bridge Isolated AC-DC Converter», 2019 IEEE Applied Power Electronics Conference and Exposition (APEC), 2019, pp. 2021-2028. doi: 10.1109/APEC.2019.8722294.

[7] M. R. Rogina et al., «Design and operation of a DC/DC converter to integrate energy storage into a railway traction system», 2021 23rd European Conference on Power Electronics and Applications (EPE'21 ECCE Europe), 2021, p. P.1-P.9. doi: 10.23919/EPE21ECCEEurope50061.2021.9570470.

[8] M. Youssef, J. A. A. Qahouq, M. Orabi, «Analysis and design of LCC resonant inverter for the tranportation systems applications», 2010 Twenty-Fifth Annual IEEE Applied Power Electronics Conference and Exposition (APEC), 2010, pp. 1778-1784. doi: 10.1109/APEC.2010.5433474.

[9] A.-Y. Ko, S.-Y. Kang, I.-K. Won, J. Yi, C.-Y. Won, «Development of a Resonant Auxiliary Power Supply Control Algorithm and Resonant Destruction Detecting for Railway Vehicles», Energies (Basel), vol. 15, n. 21, p. 8029, 2022.

[10] P. Ellams, Resonant DC Link Converters and Their Use in Rail Traction Applications. University of Salford, 1994.

[11] F. Alkayal, J. B. Saada, «Compact three phase inverter in Silicon Carbide technology for auxiliary converter used in railway applications», 2013 15th European Conference on Power Electronics and Applications (EPE), 2013, pp. 1-10. doi: 10.1109/EPE.2013.6631779.